SHIMADZU
Excellence in Science

Application Note

No. 52

Metal Materials

Evaluation of Dynamic Deformation Behavior of LPSO Type Magnesium Alloy by AE Method and High Speed Camera

Takayuki Shiraiwa [*1], Manabu Enoki [*1] and Fumiaki Yano [*2]

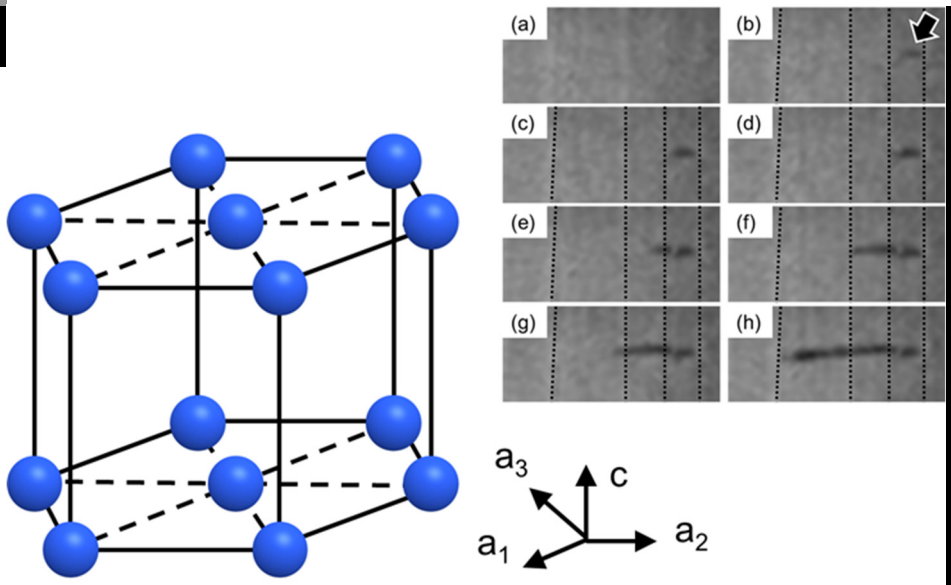

1. Introduction

In recent years, reduction of the weight of transportation machinery to improve fuel consumption has been desired from the viewpoint of global warming and other environmental problems. One proposed solution is use of magnesium alloys, which are lighter in weight than other structural materials. The density of magnesium is 1.73 g/m^3, which is the lowest among practical metal materials, being about 2/3 that of aluminum and 1/4 that of steel. Magnesium also has the advantages of superior specific strength, specific proof stress, vibration damping capacity, heat dissipation, dimensional stability, electromagnetic shielding capacity, machinability, and recyclability. However, because general magnesium alloys have a hexagonal closest-packed structure (HCP crystal structure), as shown in Fig. 1, large-scale plastic deformation at room temperature is not as easy as with other crystal structures. Moreover, the mechanical properties of magnesium alloys are not significantly superior to those of aluminum alloys. Due to these issues, little progress has been made in practical application.

The Long-Period Stacking Ordered (LPSO) type magnesium alloy, which was developed by Kawamura et al. [1)] in 2001, simultaneously achieves high strength, high heat resistance, and incombustibility, and has been an object of active research. Kawamura et al. realized the LPSO structure with $Mg_{97}Zn_1Y_2$ by the rapid solidification powder metallurgy method. The LPSO structure, as its name suggests, is a structure with a long-span atomic arrangement in comparison with conventional magnesium alloys.

It has been reported that a deformation mechanism called kink deformation occurs in microregions in this LPSO structure, and the formation of kink deformation bands is thought to contribute to high strength. Hagihara et al. [2)] performed compressions tests of unidirectionally solidified materials having a LPSO single phase structure and investigated the orientation change caused by the deformation bands. The orientation change caused by deformation bands does not take a fixed value like that in the case of twinning deformation, but rather, displays a wide distribution. Based on this, some researchers have maintained that deformation bands are caused by kink deformation and not twinning deformation. On the other hand, Kishida et al. [3)] proposed that the distinctive deformation bands formed by Mg-Al-Gd system alloys that contain the LPSO phase are not formed by kink deformation, but by twinning deformation followed by crystal rotation. Since the twins that occur here are a twin system called $\{11\bar{2}1\}$ tensile twins and have rarely been reported in magnesium and its alloys, it is possible that the LPSO structure plays a critical role in the formation of this twin system. Thus, there are still many unknown points in connection with the kink deformation of the LPSO phase, and it is necessary to elucidate the detailed behavior of this kink deformation for further alloy development of LPSO type magnesium alloys.

*1 Department of Materials Engineering, The University of Tokyo
*2 Analytical & Measuring Instruments Division, Global Application Development Center, Shimadzu Corporation

In previous work, we evaluated the dynamic deformation and fracture mechanism of various magnesium alloys by the acoustic emission (AE) method [4)-11)]. This article introduces an example of observation of kink deformation bands in a LPSO type magnesium alloy by a combination of the AE method and a high speed camera.

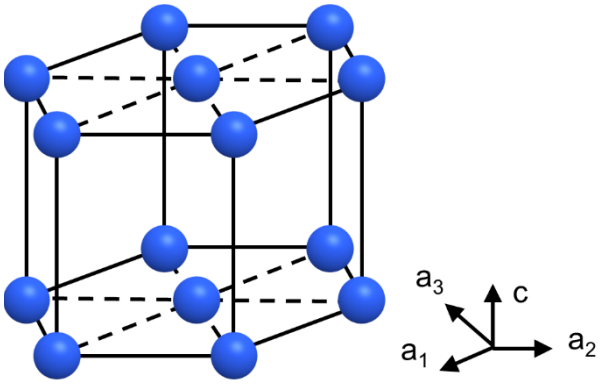

Fig. 1 Hexagonal Closest-Packed Structure (HCP Crystal Structure) of Magnesium Alloy

2. Recording Method

Cubic compression test specimens with a side length of 5 mm were prepared from unidirectionally solidified $Mg_{85}Zn_6Y_9$ material with a LPSO phase volume fraction of 97.5 %. The unidirectionally solidified material was strongly oriented so that the solidification direction and bottom surface were parallel. Fig. 2 shows a schematic diagram of the structure and SEM images. One of the side surfaces of the specimen was mirror polished to enable observation of the condition of the specimen surface after the compression test. The compression test was performed at room temperature with a crosshead speed of 5.00×10^{-4} mm/s using a Shimadzu AG-5000C Autograph™. Fig. 3 shows a schematic diagram of the measurement system and the condition of recording. The test was performed using a compression tool with a spherical seat as the top-side tool so as to minimize the alignment error of the top and bottom surfaces of the specimen. The compression direction was parallel to the solidification direction.

During the test, the specimen surface was observed at framerates of 80,000 FPS and 5,000,000 FPS using high speed cameras (Vision Research Inc., Phantom Miro M110 and Shimadzu, HPV™-X2, respectively). An AE signal was used as a trigger in order to capture the instant when deformation occurred. The trigger voltage was 500 mV or 1,000 mV.

A M304A resonance type AE sensor (Fuji Ceramics Corp.) was used as the AE sensor. After polishing the contact surfaces in the top and bottom tools with abrasive paper, the AE sensors were glued to the tools with Aron Alpha® Superset (Konishi Co., Ltd.). The signal from the measuring AE sensor was amplified by an A1001 preamplifier (Fuji Ceramics) and recorded using Continuous Wave Memory [12)], which enables continuous waveform measurement. The AE measurements were performed with a sampling rate of 10 MHz and a measurement range of ±5000 mV.

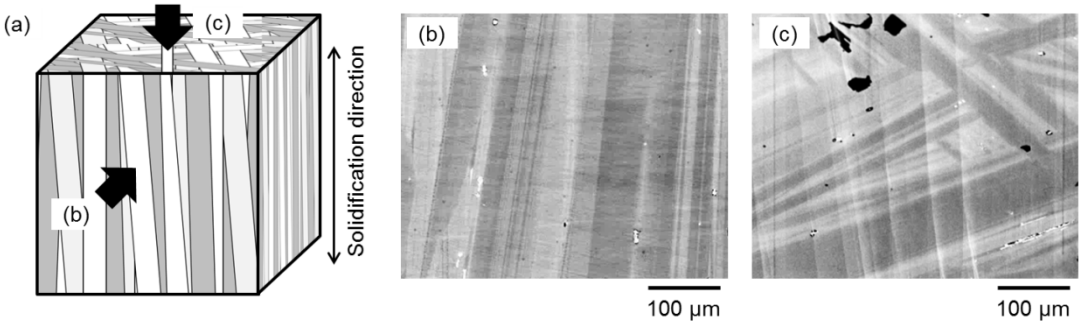

Fig. 2 Structure of Unidirectionally Solidified $Mg_{85}Zn_6Y_9$ Material: (a) Schematic Diagram, (b) Surface Parallel to Solidification Direction, and (c) Surface Perpendicular to Solidification Direction

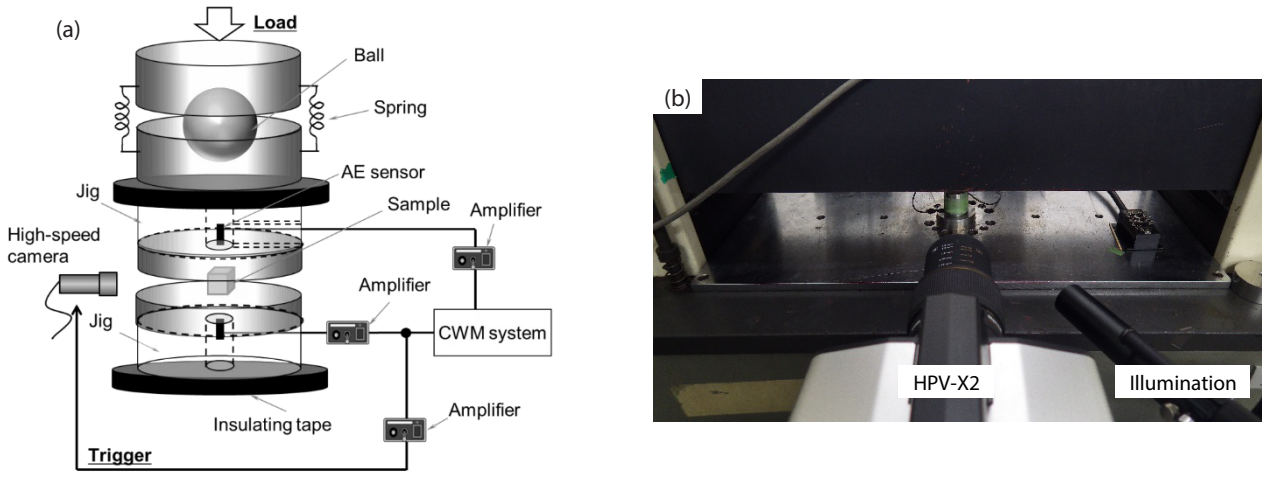

Fig. 3 Measurement System Used in Compression Test of Magnesium Alloy: (a) Schematic Diagram and (b) Condition of Recording

3. Recording Results

It was possible to observe a total of 8 kink deformation bands by using the AE signal caused by kink deformation as a trigger. Fig. 4 shows a kink deformation band recorded at a frame rate of 20,000 FPS (temporal resolution: 50 μs) using a conventional high speed camera. Although no change has occurred in the first frame, formation of a kink deformation band in that part can be confirmed in the second frame, and expansion of the deformation band can be observed in the third frame. This showed that formation of the kink deformation band occurred in 50 μs or less, and suggested that observation at a higher speed is necessary in order to capture the dynamic process from initiation to expansion of deformation bands. Therefore, formation of kink deformation bands was recorded with the Shimadzu HPV-X2 high speed camera, which enables recording at a framerate of 5,000,000 FPS (temporal resolution: 0.2 μs). Fig. 5 shows the images obtained with the Shimadzu high speed camera. The dotted lines in the figure indicate grain boundaries. A condition in which a kink deformation band occurred and then grew during one 0.2 μs frame was confirmed. Growth then proceeded by a repeated process in which growth stopped temporarily at a grain boundary, resumed, and then stopped again at the next grain boundary. In comparison with deformation band formation, the observation results showed that the growth process is a phenomenon with a long time span. As described above, dynamic observation of kink deformation bands was possible by using an AE signal as a trigger.

The AE waveforms measured during the test were classified into two clusters based on their frequency components. Cluster 1 displayed high AE energy on the low frequency side, while cluster 2 displayed high AE energy on the high frequency side. Fig. 6 shows the area ratio of the kink deformation bands and the number of grains with one or more kink deformation bands, together with the stress curve and the curves of the cumulative number of AE events in each cluster. The number of grains with one or more deformation bands showed behavior consistent with AE cluster 1. In a tensile test of an AZ system magnesium alloy, Yasutomi et al. [8] showed that high AE energy occurs in initial twin formation. Likewise, in the present research, high AE energy occurred in the kink deformation, which occurred in the initial stage, and the AE events at that time were extracted and classified in the cluster 1. Based on these facts, the main source of AE in cluster 1 is considered to be kink deformation in the initial stage of deformation. Next, Fig. 7 shows the number of micro cracks, together with the stress curve and the curves of the cumulative number of AE events in each cluster. The behavior of the number of micro cracks shows good agreement with the behavior of the cumulative number of AE events belonging to AE cluster 2. From this, the main AE source of cluster 2 is considered to be micro cracks. The moment of the AE sources was obtained by back analysis of the AE waveforms. Based on several hypotheses, the dimensions of the kink deformation bands were estimated from the relational expression of the moment and eigenstrain. The results were in good agreement with the actual dimensions of the kink deformation bands. (For details, refer to Reference [11].)

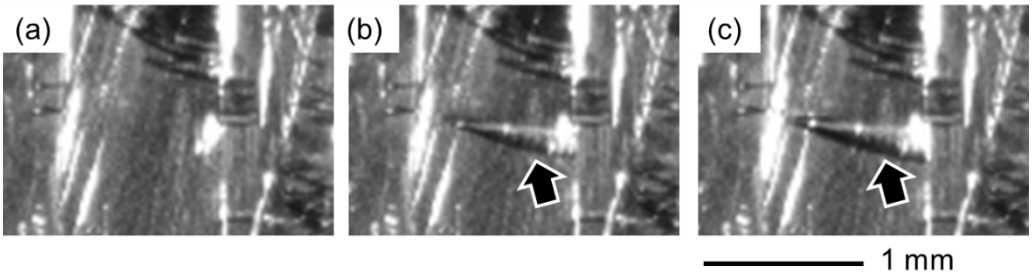

Fig. 4 Observation of Kink Deformation by Conventional High Speed Camera (Framerate: 20,000 FPS): (a) 0 μs, (b) 50 μs, (c) 100 μs

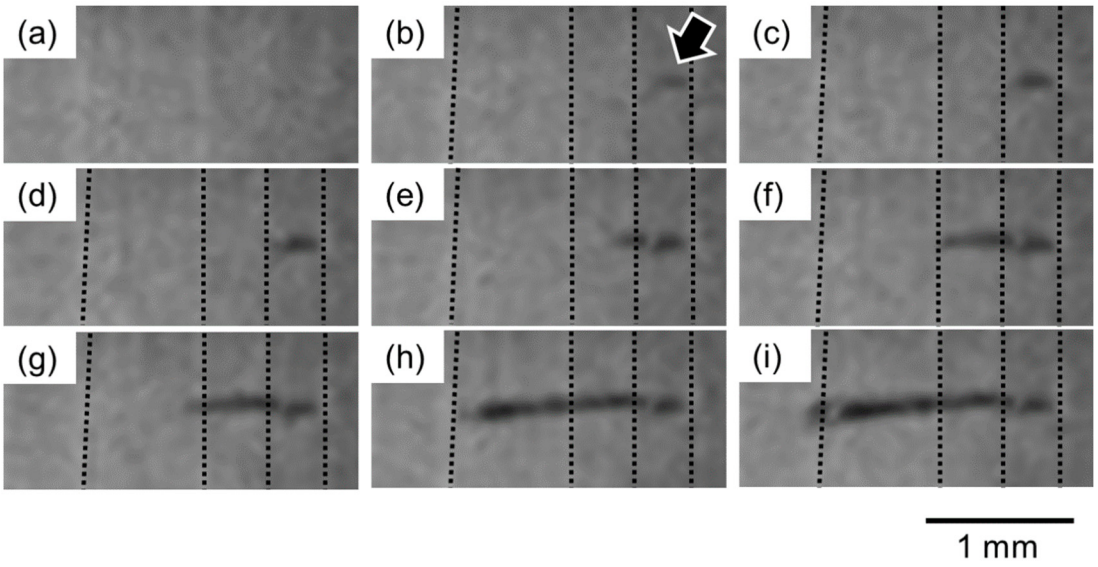

Fig. 5 Observation of Kink Deformation by Shimadzu High Speed Camera (Framerate: 5,000,000 FPS): (a) 0 µs, (b) 0.2 µs, (c) 0.4 µs, (d) 2.0 µs, (e) 2.4 µs, (f) 3.0 µs, (g) 5.0 µs, (h) 6.4 µs, (i) 8.0 µs. The dotted lines indicate grain boundaries.

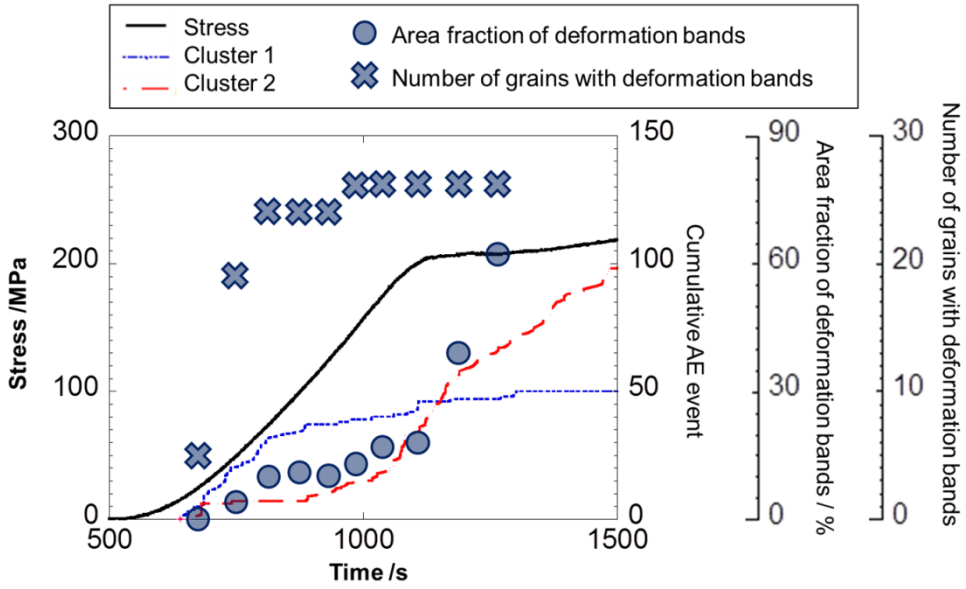

Fig. 6 Area Fraction of Kink Deformation Bands, Number of Grains with Deformation Bands, and Time Change in Cumulative Number of AE Events

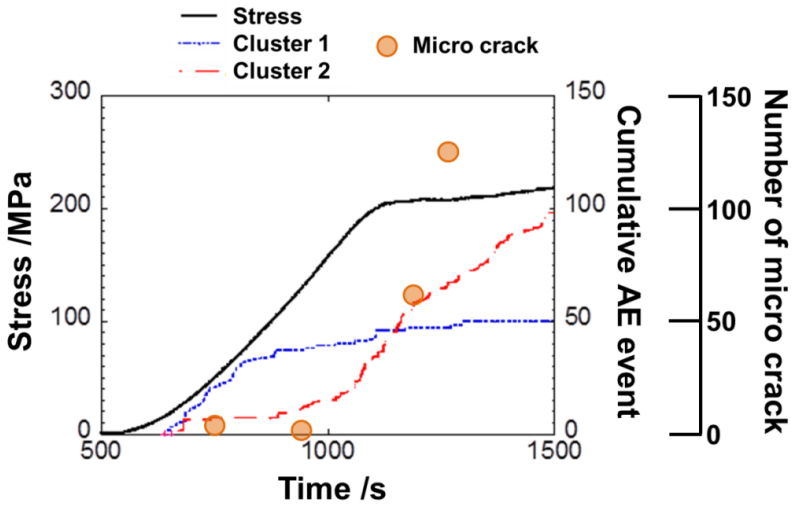

Fig. 7 Number of Micro Cracks and Time Change in Cumulative Number of AE Events

4. Conclusion

This article introduced an example of observation of kink deformation bands with a high speed camera. In research and development of structural materials, observation and analysis of dynamic deformation behavior are necessary and indispensable. The AE method is almost the only method that can capture the internal dynamic behavior of materials in real time. However, because AE is an indirect evaluation method and the main observation region is the ultrasonic region from 100 kHz to 2 MHz, direct observation of the actual phenomena at the AE generation source was difficult with conventional techniques, even when using a high speed camera. As a result of improvement in the performance of high speed cameras in recent years, a framerate of 10,000,000 FPS and high photosensitivity can now be achieved simultaneously, enabling observation of the actual phenomena at substantially the same sampling rate as that in AE measurement.

As introduced in this article, it is expected to be possible to capture phenomena that could not be observed until now by using a combination of direct observation of the material surface by a high speed camera and in-situ observation of dynamic behavior, including the interior of the material, by AE analysis. Since this is considered to be an extremely powerful technique, not only for observation of kink deformation bands, but also for elucidation of a variety of other dynamic behaviors, including phase transformation and fracture phenomena such as crack initiation and growth, further expansion of applications as a research technique is expected.

References

1) Y. Kawamura, K. Hayashi, A. Inoue and T. Masumoto: Mater. Trans., **42** (2001) 1172-1176.
2) K. Hagihara, M. Yamasaki, M. Honnami, H. Izuno, M. Tane, T. Nakano and Y. Kawamura: Philos. Mag., **95** (2015) 132-157.
3) K. Kishida, A. Inoue, H. Yokobayashi and H. Inui: Scripta Mater., **89** (2014) 25-28.
4) Y. P. Li and M. Enoki: Mater. Trans., **48** (2007) 1215-1220.
5) Y. P. Li and M. Enoki: Mater. Trans., **48** (2007) 2343-2348.
6) Y. P. Li and M. Enoki: Mater. Trans., **49** (2008) 1800-1805.
7) Y. P. Li and M. Enoki: Mater. Sci. Eng. A, **536** (2012) 8-13.s
8) T. Yasutomi and M. Enoki: Mater. Trans., **53** (2012) 1611-1616.
9) Y. Muto, K. Matsumoto, T. Shiraiwa and M. Enoki: J. Japan Inst. Metals, **78** (2014) 381-387.
10) Y. Muto, T. Shiraiwa and M. Enoki: J. Japan Inst. Metals, **80** (2017) 697-701.
11) Y. Muto, T. Shiraiwa and M. Enoki: Mater. Sci. Eng. A, **689** (2017) 157-165.
12) K. Ito and M. Enoki: Mater. Trans., **48** (2007) 1221-1226.

First Edition: Nov. 2018

SHIMADZU

Shimadzu Corporation

www.shimadzu.com/an/

Related Solutions

- Electronics

- Price Inquiry
- Product Inquiry
- Technical Service / Support Inquiry
- Other Inquiry